

lncRNA UCA1 Predicts a Poor Prognosis and Regulates Cell Proliferation and Migration by Repressing p21 and SPRY1 Expression in GC

Xuezhi He,^{1,8} Jing Wang,^{1,7,8} Jin Chen,^{2,8} Liang Han,^{3,8} Xiyi Lu,¹ Dengshun Miao,^{1,7} Dandan Yin,⁴ Qinghe Geng,⁵ and Erbao Zhang^{6,7}

¹Department of Anatomy, Histology and Embryology, The Research Center for Bone and Stem Cells, Nanjing Medical University, Nanjing, Jiangsu, People's Republic of China; ²The Fourth Clinical Medical College, Nanjing Medical University, Nanjing, Jiangsu, People's Republic of China; ³Department of Oncology, Xuzhou Central Hospital, The Xuzhou School of Clinical Medicine of Nanjing Medical University, Nanjing Medical University, Nanjing, Jiangsu, People's Republic of China; ⁴Department of Clinical Research Center, Nanjing Second Hospital, Nanjing University of Chinese Medicine, Nanjing, Jiangsu, People's Republic of China; ⁵Department of General Surgery, Pizhou City People's Hospital, Pizhou City 221300, Jiangsu Province, China; ⁶Department of Epidemiology and Biostatistics, Jiangsu Key Lab of Cancer Biomarkers, Prevention and Treatment, Collaborative Innovation Center for Cancer Personalized Medicine, School of Public Health, Nanjing Medical University, Nanjing, Jiangsu, People's Republic of China; ⁷State Key Laboratory of Reproductive Medicine, Nanjing Medical University, Nanjing, Jiangsu, People's Republic of China

Dysregulated expression of long non-coding RNAs (lncRNAs) has been reported in many types of cancers, indicating that it has important regulatory roles in human cancer biology. Recently, lncRNA urothelial cancer-associated 1 (UCA1) was shown to be dysregulated in many cancer types, but the detailed mechanisms remain largely unknown. In our study, we found that upregulated UCA1 is associated with poor prognosis in gastric cancer patients. Further experiments revealed that UCA1 knockdown significantly repressed the proliferation and migration both *in vitro* and *in vivo*. Moreover, RNA sequencing (RNA-seq) analysis revealed that UCA1 knockdown preferentially affected genes that are linked to cell proliferation, cell cycle, and cell migration. Mechanistically, UCA1 promotes cell proliferation progression through repressing p21 and Sprouty RTK signaling antagonist 1 (SPRY1) expression by binding to EZH2. We found that UCA1 could mediate the trimethylation of H3K27 in promoters of p21 and SPRY1. To our knowledge, this is the first report showing the global gene profile of downstream targets of UCA1 in the progression of gastric cancer. Collectively, our data reveal the important roles of UCA1 in gastric cancer (GC) oncogenesis.

INTRODUCTION

Gastric cancer (GC) is one of the most common malignancies and a major cause of cancer-related death worldwide due to the limited therapeutic options, tumor metastasis, and the high frequency of tumor recurrence.¹ In spite of the advances in diagnostic and surgical techniques and molecular targeting therapy, the 5-year overall survival rate for GC patients remains poor.² The clinical stage, based on the tumor node metastasis (TNM) classification system, at the time of diagnosis is currently the most important prognostic factor.

Furthermore, the molecular mechanism involved in progression and metastasis of gastric cancer remains poorly understood.³ Therefore, a better understanding of the molecular mechanisms underlying gastric carcinoma pathogenesis and progression is essential for the development of diagnostic markers and novel effective therapies for GC patients.

Recently, one of the most important discoveries at the genomic scale is that there are much more abundant non-coding transcripts in different species than previously imagined. Long noncoding RNAs (lncRNAs) are defined as transcripts longer than 200 nt without coding capacities. lncRNAs have appealed to a large group of researchers and become a main focus of attention. lncRNAs are now known to have many functions, acting as scaffolds or guides to regulate interactions between protein and genes, as decoys to bind proteins or microRNAs (miRNAs), and as

Received 24 May 2019; accepted 18 September 2019;
<https://doi.org/10.1016/j.omtn.2019.09.024>

⁸These authors contributed equally to this work.

Correspondence: Dengshun Miao, Department of Anatomy, Histology and Embryology, The Research Center for Bone and Stem Cells, Nanjing Medical University, Nanjing, Jiangsu, People's Republic of China.
E-mail: dsmiao_edu@sohu.com

Correspondence: Dandan Yin, Department of Clinical Research Center, Nanjing Second Hospital, Nanjing University of Chinese Medicine, Nanjing, Jiangsu, People's Republic of China.
E-mail: jsnydandan@sina.com

Correspondence: Qinghe Geng, Department of General Surgery, Pizhou City People's Hospital, Pizhou City 221300, Jiangsu Province, China.
E-mail: qinghegengsohuco@sohu.com

Correspondence: Erbao Zhang, Department of Epidemiology and Biostatistics, Jiangsu Key Lab of Cancer Biomarkers, Prevention and Treatment, Collaborative Innovation Center for Cancer Personalized Medicine, School of Public Health, Nanjing Medical University, Nanjing, Jiangsu 211166, People's Republic of China.
E-mail: erbaozhang@njmu.edu.cn



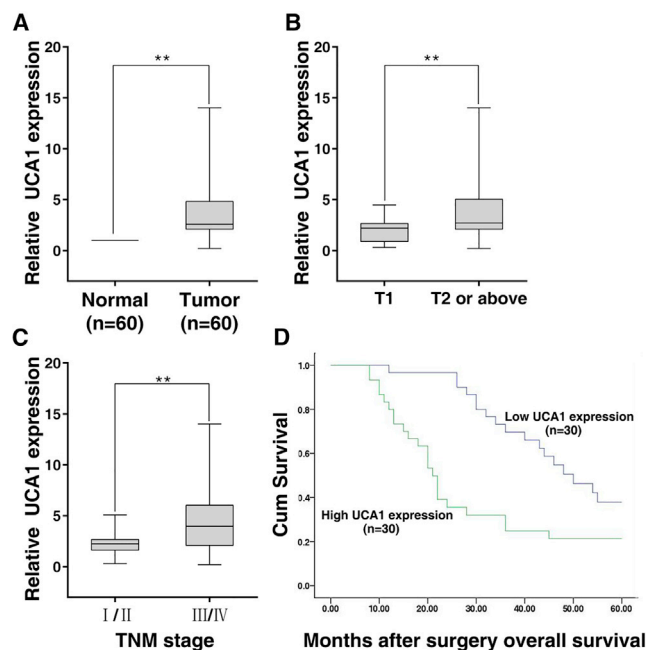


Figure 2. UCA1 Expression Is Increased in Human Gastric Cancer Tissues and Correlates with Poor Prognosis

(A) UCA1 expression was inspected by qRT-PCR and normalized to GAPDH expression in human gastric tissues compared with corresponding non-tumor tissues ($n = 60$). (B and C) UCA1 expression was significantly higher in patients with deeper invasion depth (B) and advanced TNM stage (C). (D) We divided the samples into high (above the median, $n = 30$) and low (below the median, $n = 30$) UCA1 expression groups according to median value of UCA1 levels. Patients with high levels of UCA1 expression are less likely to survive compared with low expression of UCA1 ($p < 0.001$, log-rank test; * $p < 0.05$, ** $p < 0.01$).

Next, we used qRT-PCR to detect UCA1 expression in 60 paired gastric cancer samples and adjacent normal tissues. As shown in Figure 2A, UCA1 was significantly overexpressed in 60 paired GC tissues. Furthermore, we explored the correlation between UCA1 expression and the clinical-pathological factors of patients with GC. In general, UCA1 level was associated with invasion depth and TNM stage. Specifically, patients with deeper invasion depth or advanced TNM stage (III/IV) were associated with a higher UCA1 expression, whereas patients with shallower invasion depth or local TNM stage (I/II) were associated with a lower UCA1 level (Figures 2B and 2C).

In addition, we divided the samples into high (above the mean, $n = 30$) and low (below the mean, $n = 30$) UCA1 expression groups, according to the median value of UCA1 levels. A chi-square test was performed to evaluate clinical-pathological factors between the two groups. Next, we attempted to evaluate the correlation between UCA1 expression and clinical outcomes. Kaplan-Meier analysis and the log-rank test were used to evaluate the effects of UCA1 expression and the clinicopathological characteristics on overall survival (OS). The median survival time for low UCA1 expression groups was 44.162 ± 2.442 months, while that for high UCA1 expression groups

was only 30.646 ± 2.507 months. As shown in Figure 2D, overexpression of UCA1 predicted a poor prognosis in patients with GC ($p < 0.01$). In addition, univariate survival analysis showed that TNM stage, lymph node metastasis, tumor differentiation, and UCA1 expression level were significantly associated with the OS of patients. Multivariate Cox regression analyses showed that TNM stage ($p = 0.025$) and lymph node metastasis ($p = 0.024$) were independent prognostic factors for gastric cancer patients (Table S1).

Knock Down of UCA1 Impaired GC Cell Proliferation and Migration *In Vitro*

To investigate the biological functions of UCA1 in gastric cancer cells, we first detected the expression of UCA1 in a normal human gastric mucosa cell line (GES-1) and diverse human GC cell lines using qRT-PCR analysis. As shown in Figure S1A, UCA1 expression was significantly upregulated in two GC cell lines (BGC-823 and SGC-7901) compared with GES-1. Thus, the BGC-823 and SGC-7901 cell lines were chosen for further study. Next, we performed knock down of UCA1 in BGC-823 and SGC-7901 cells by transfecting them with small interfering RNA (siRNA) (Figure S1B). Then MTT assays showed that knock down of UCA1 expression significantly inhibited cell proliferation compared with the control cells (Figure 3A). Similarly, the result of a colony formation assay revealed that clonogenic survival of BGC-823 and SGC-7901 cells was significantly impaired following the knock down of UCA1 (Figure 3B). EdU staining assays also showed that decreased UCA1 expression inhibited BGC-823 and SGC-7901 cell proliferation (Figure 3C).

Next, transwell assays were performed to investigate the role of UCA1 on gastric cancer cell migration ability. The results revealed that knock down of UCA1 significantly repressed cell migration compared with the control cells (Figure 3D). These results indicated that knock down of UCA1 had tumor-suppressive effects that could inhibit migration in GC cells.

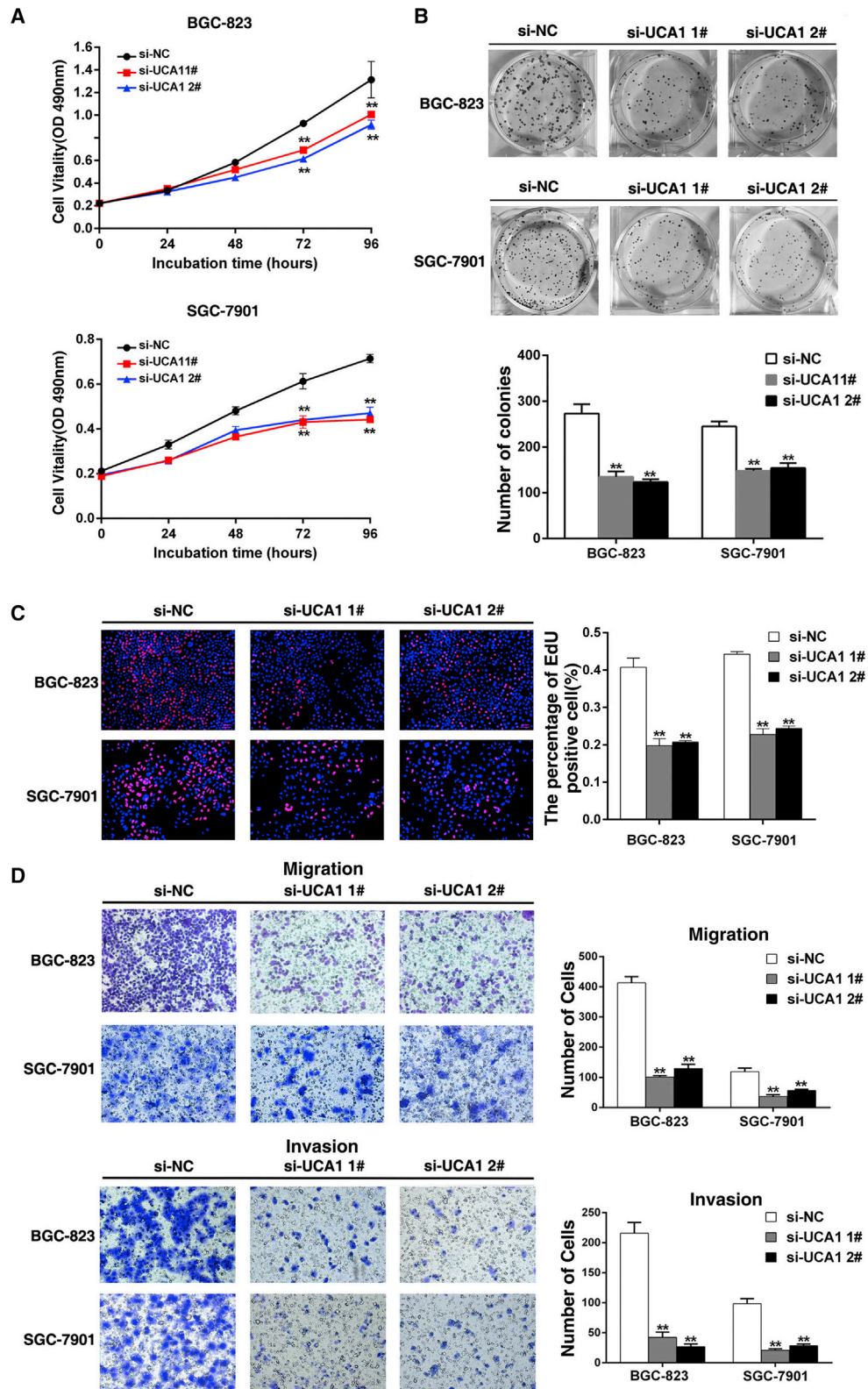
Knock Down of UCA1 Could Induce Cell-Cycle Arrest and Apoptosis of Gastric Cancer Cells

To examine whether the effect of UCA1 on the proliferation of GC cells reflected cell-cycle arrest, cell cycle progression was analyzed by flow cytometry analysis. The results revealed that BGC-823 and SGC-7901 cells transfected with si-UCA1 had an obvious cell-cycle arrest at the G1/G0 phase and a decreased G2/S phase (Figure 4A).

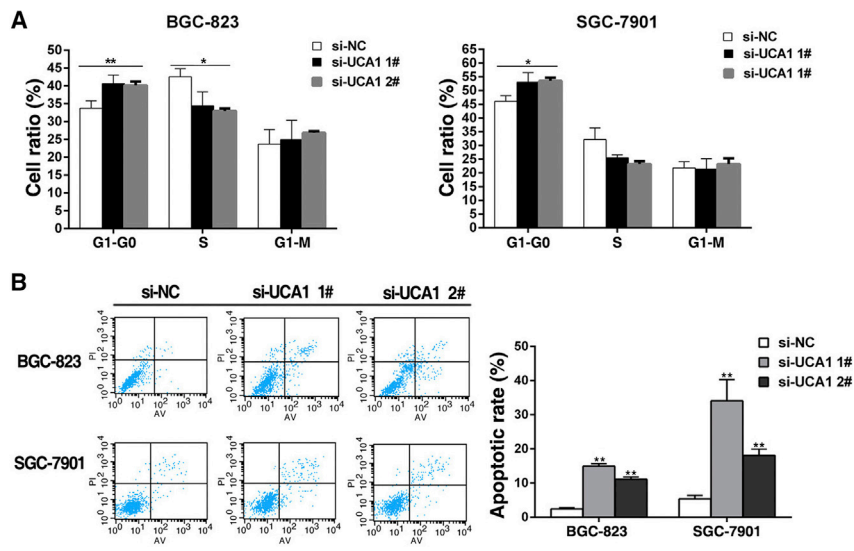
To further determine whether GC cell proliferation was influenced by cell apoptosis, we performed flow cytometry analysis. The results showed that GC cells transfected with UCA1 siRNA showed a higher apoptotic rate in comparison with control cells (Figure 4B). Collectively, these data indicate that UCA1 exerts an oncogenic effect to promote the proliferation of GC cells.

UCA1 Regulated GC Cell Proliferation and Migration *In Vivo*

We next explored the role of UCA1 in tumor-initiating formation of GC *in vivo*. We performed subcutaneous injection of BALB/c nude mice with stable knock down of sh-UCA1 and shCtrl BGC-823 cells.



(legend on next page)



At 16 days after the injection, the tumors that formed in the sh-UCA1 group were substantially smaller than those in the control group (Figures 5A and 5C). Moreover, the mean tumor weight at the end of the experiment was markedly lower in the sh-UCA1 group compared with the control vector group (Figure 5B). Tumors formed from stably sh-UCA1-transfected BGC-823 cells exhibited decreased positivity for Ki-67 than those from control cells (Figure 5D). These findings indicate that knock down of UCA1 inhibits tumor growth *in vivo*.

To validate the effects of UCA1 on the metastasis of SGC-7901 cells *in vivo*, SGC-7901 cells stably transfected with sh-UCA1 or control vector were injected into the tail veins of nine mice. Metastatic nodules on the surface of the lungs were counted after 7 weeks. Knock down of UCA1 reduced the number of metastatic nodules compared with the control group (Figure 5E). This difference was further confirmed following the examination of the entire lungs and through H&E staining of lung sections. Our *in vivo* data therefore complemented the results of functional *in vitro* studies involving UCA1.

The Global Gene Expression Profile Mediated by UCA1

To analyze the UCA1-associated gene transcriptional changes, we performed RNA transcriptome sequencing to assess the gene expression profiles of control or siRNAs against UCA1. The results showed that the expressions of 308 genes were upregulated (\log_2 fold change ≥ 2) and those of 222 genes were downregulated ($|\log_2$ fold change| ≥ 2) (Figure 6A; Table S2) in BGC-823 cells with UCA1 knockdown compared with that in control cells. Gene Ontology (GO) analysis showed that these genes are involved in the biological processes of cell proliferation, cell cycle, and cell adhesion among

Figure 4. Knock Down of UCA1 Induced Cell-Cycle Arrest and Apoptosis of Gastric Cancer Cells

(A) At 48 h after transfection, cell cycle was analyzed by flow cytometry. The bar chart represents the percentage of cells in G1-G0, S, or G2-M phase, as indicated. (B) Flow cytometry was performed to detect the apoptotic rates of BGC-823 and SGC-7901 cells after UCA1 knockdown. LR, early apoptotic cells; UR, terminal apoptotic cells. * $p < 0.05$, ** $p < 0.01$.

others (Figure 6A). Several upregulated or down-regulated genes that contribute to gastric cancer were selected and confirmed by qPCR assays (Figure 6B). Among these genes, p21 attracted our attention because of its established tumor suppressor role in tumorigenesis and its being involved in the cancer cell cycle.²⁴ In addition, SPYR1 has been identified as a tumor suppressor that is involved in cancer cell proliferation, apoptosis, and invasion.²⁵ Hence, we chose p21 and SPYR1 for further investigation.

UCA1 Epigenetically Suppressed p21 and SPYR1 Transcription by Interacting with EZH2

To explore the mechanism for UCA1-mediated regulation, here we first analyzed the distribution of the UCA1 transcript in GC cells, and we found that it mostly localized in the nucleus, which suggested that it plays a major regulatory function at the transcriptional level (Figure 7A).

Recent studies have reported that a larger number of lncRNAs have been identified to function in cooperation with PRC2 (polycomb repressive complex 2) to promote epigenetic activation or silencing of gene expression, especially in cancer.^{26–28} PRC2, a methyltransferase that is composed of EZH2, SUZ12, and EED, can catalyze the di- and trimethylation of lysine residue 27 of histone 3 (H3K27me3), thus epigenetically modulating gene expression.²⁹ Approximately 20% of all human lncRNAs have been shown to physically associate with PRC2, suggesting that lncRNAs may have a general role in recruiting polycomb group proteins to their target genes.³⁰ In addition, aberrations in PRC2 are closely related to carcinogenesis.³¹ Previous research found that UCA1 could bind to EZH2.²⁰

To determine whether UCA1 regulates the potential targets through binding to EZH2 in GC cells, we performed RNA immunoprecipitation (RIP) assays for EZH2 and SUZ12 in GC cells. The results showed that UCA1 could bind with EZH2 and SUZ12, but its interaction with EZH2 was stronger; whereas HOTAIR, which could bind to PRC2, was used as positive control (Figure 7B). Moreover, we

Figure 3. Effects of UCA1 on Gastric Cell Proliferation and Cell Cycle Progression In Vitro

(A) MTT assays were used to determine the viability of UCA1 knockdown in BGC-823 and SGC-7901 cells by using siRNAs. (B) Colony formation assays were performed to determine the cell proliferation of UCA1 knockdown in BGC-823 and SGC-7901 cells. (C) Proliferating BGC-823 and SGC-7901 cells were labeled with EdU (red); cell nuclei were stained with DAPI (blue). (D) Transwell assays were used to determine the changes in migratory and invasive abilities of gastric cancer cells. ** $p < 0.01$.

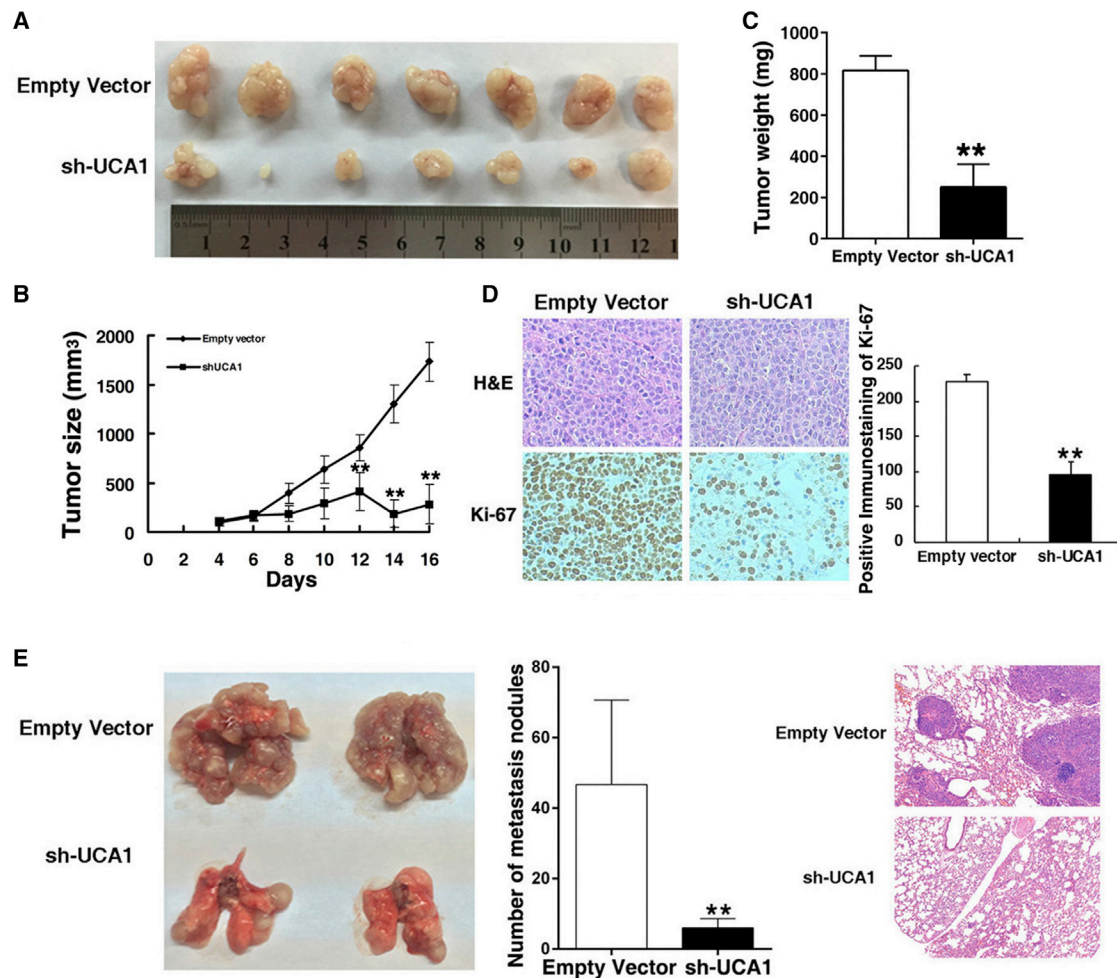


Figure 5. UCA1 Regulates Tumorigenesis and Metastasis of Gastric Cancer Cells *In Vivo*

(A) The nude mice were injected with BGC-823 cells, which were transfected with empty vector or sh-UCA1, respectively. Tumors formed in the sh-UCA1 group were smaller than those in the control group. (B) Tumor volumes were calculated after injection every 3 days. (C) Tumor weights were represented as means of tumor weights \pm SD. (D) The tumor sections were under H&E staining and IHC staining using antibodies against Ki-67. (E) The analysis of an experimental metastatic animal model was transferred steadily UCA1 to the nude mouse by injecting SGC-7901 cells. Lungs from mice in each experimental group, with the numbers of tumor nodules on lung surfaces, are shown. Visualization is of the entire lung and H&E-stained lung sections. * $p < 0.05$, ** $p < 0.01$.

found that knock down of UCA1 did not affect the expression of EZH2 (Figure S2A), and knock down of EZH2 could inhibit cell proliferation and migration in BGC-823 cells (Figures S2B–S2D). Together, these results demonstrated a specific association between EZH2 and UCA1.

Then the role of EZH2 in the suppression of UCA1-suppressed genes was investigated by EZH2 knockdown. As shown in Figure 8A, we first transiently depleted the expression of EZH2 in BGC-823 and SGC-7901 cells. In addition, we observed that the loss of UCA1/EZH2 was associated with the upregulation of p21 and SPYR1 at the mRNA and protein levels (Figure 8B). We then performed chromatin immunoprecipitation (ChIP) assays to examine the regulatory mechanisms. Our results found that knock down of UCA1 decreased the binding of EZH2 and H3K27 trimethylation levels across the pro-

motors of p21 and SPYR1, confirming that p21 and SPYR1 were bona targets of UCA1-regulated genes (Figure 8C). These results suggest that UCA1 affects GC cell growth and metastasis at least partly through the epigenetic repression of p21 and SPYR1, by interacting with EZH2.

DISCUSSION

In the past decade, the functions of lncRNAs have been less understood compared to short ncRNAs. lncRNAs played a vital role in the regulation of human normal development and differentiation.^{32,33} Dysregulated lncRNA expression was associated with disease generation and development, including cancer progression.^{34,35} For example, our previous work found that CCAT1 could regulate cell proliferation and migration in esophageal squamous cell carcinoma.³⁴ A large number of lncRNAs was expressed disorderly

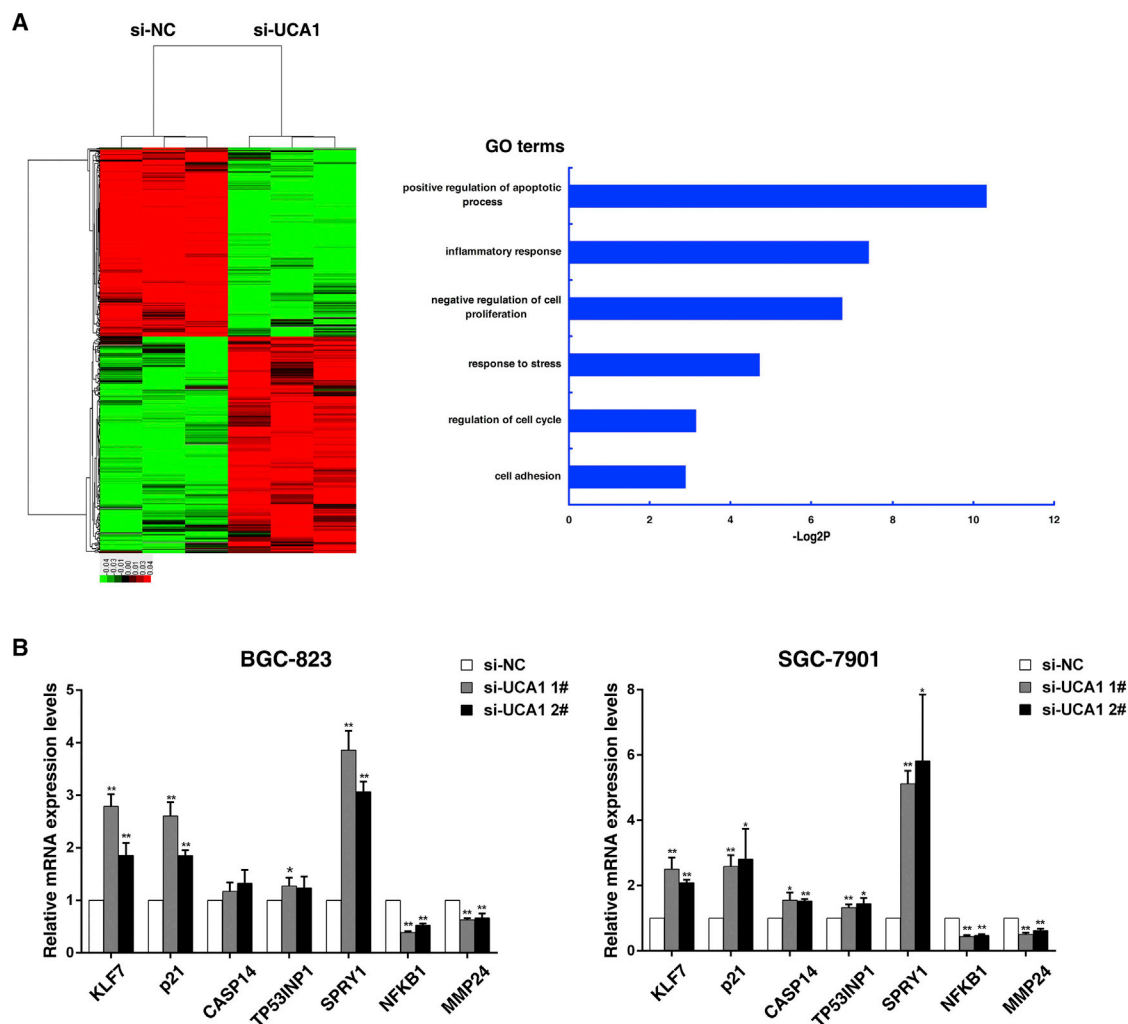


Figure 6. RNA-Seq after UCA1 Knockdown in BGC-823 Cells

(A) Mean-centered, hierarchical clustering of genes altered (≥ 2 -fold change) in si-NC-treated cells and siRNA-UCA1-treated cells, with three repeats. Gene ontology analysis for all genes with altered expressions. (B) The altered mRNA levels of genes were selectively confirmed by qRT-PCR in knockdown UCA1. * $p < 0.05$, ** $p < 0.01$.

in gastric cancer and acted as oncogenes or cancer suppressors, which opens avenues for the use of lncRNAs in the identification and treatment of novel diagnostic or predictive biomarkers and targets.

For instance, our previous study showed that HOTAIR could also function as a competing endogenous RNA by sponging miR-331-3p.³⁶ We also found that a novel lncRNA, HOXC-AS3, is upregulated in gastric cancer and regulates cell proliferation and migration by binding to YBX1.³⁷ In this study, we analyzed the expression levels of UCA1 in human gastric cancer tissues by using raw microarray data downloaded from GEO (GEO: GSE118897) and TCGA. We discovered that the UCA1 expression levels were upregulated in gastric cancerous tissues compared with noncancerous tissues. Meanwhile, high UCA1 expression in gastric cancer was significantly correlated with advanced TNM stage,

lymph node metastasis, tumor differentiation, and patients' prognosis. More importantly, there has been no study that revealed the molecular mechanism and downstream targets of UCA1 in GC until now.

Here we demonstrated that the knock down of UCA1 inhibited gastric cancer cell proliferation and metastasis and promoted cell apoptosis. The results of animal experiments showed that the knock down of UCA1 suppressed gastric cancer cell tumorigenesis and metastasis *in vivo*. The results of RNA-seq with GO analysis showed that UCA1 regulates proliferation and apoptosis-related gene expression after UCA1 knockdown in gastric cancer cells. Furthermore, this study provided evidence for the first time that UCA1 exerted oncogenic functions in human GC cells by interacting with EZH2 and repressing p21 and SPYR1 expressions, thus regulating the proliferation and metastasis of gastric cancer.

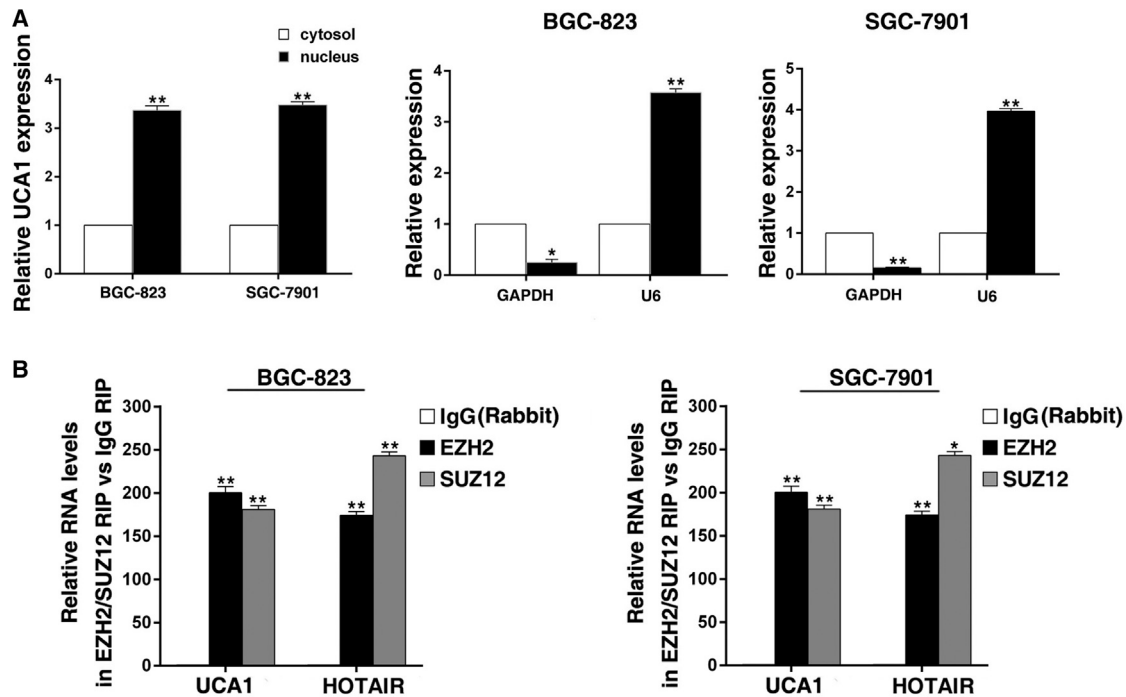


Figure 7. UCA1 Could Directly Bind with EZH2

(A) After nuclear and cytosolic separation, RNA expression levels were measured by qRT-PCR. GAPDH was used as a cytosol marker and U6 was used as a nucleus marker. (B) RIP experiments were performed in BGC-823 and SGC-7901 cells, and the coprecipitated RNA was subjected to qRT-PCR for UCA1. HOTAIR was used as a positive control. The fold enrichment of UCA1 in EZH2 RIP is relative to its matching immunoglobulin G (IgG) control RIP. * $p < 0.05$, ** $p < 0.01$.

As a target of UCA1, p21 is a cyclin-dependent kinase (CDK) inhibitor. It is downregulated in a variety of cancer types and plays critical roles in multiple cellular processes during unperturbed cell growth.^{38,39} It could inhibit cell proliferation in normal and cancer cells by inhibiting the activity of kinases related to G1/S transition, such as CyclinD/CDK4, CyclinD/CDK6, and CyclinE/CDK2.^{40,41} In addition, PRC2-mediated histone methylation contributes to the repression of p21.⁴²

As another target of UCA1, SPRY1, as part of the mammalian Sprouty gene family consisting of four members (SPRY1–4), may have a tumor suppressor function in specific tumors, as its expression is downregulated in several human cancers, such as prostate and breast cancers.^{43–45} Subsequent studies showed that the overexpression of SPRY1 inhibited cell proliferation, migration, and invasion in tumor cell lines.^{46,47} However, so far very little is known about the specific functional role and the mechanism of this gene in GC. Moreover, previous studies have found that DNA methylation in the SPRY1 promoter region is responsible for downregulating SPRY1 expression.^{47,48} Our results found that histone methylation (H3K27me3) mediated by UCA1 could also contribute to the lower expression of SPRY1 in gastric cancer. In addition, studies have reported that histone methylation usually cooperates with DNA methylation in heritable repression of gene activity.^{49–52} Here we provide the evidence that the transcriptional regulation of p21 and SPRY1 is partly mediated by UCA1 in the tumor progression of

GC, through interacting with EZH2, thus facilitating GC cell proliferation and metastasis.

In summary, we have shown that UCA1 expression was upregulated in GC tissues, suggesting that its upregulation may be a negative prognostic factor for GC patients. Moreover, UCA1 could regulate gastric cancer cell proliferation and metastasis both *in vitro* and *in vivo*. As for the underlying molecular mechanism, UCA1 mediated the oncogenic effects partially through its epigenetic silencing of the p21 and SPRY1 expressions by binding to EZH2. Our findings further the understanding of GC pathogenesis, and they facilitate the development of lncRNA-directed diagnostics and therapeutics against this disease.

MATERIALS AND METHODS

Tissue Collection and Ethics Statement

A total of 60 primary gastric cancer tissues was collected from patients who had undergone surgery at the First Affiliated Hospital of Nanjing Medical University and the Second Affiliated Hospital of Nanjing Medical University. The study was approved by the Ethics Committee of Nanjing Medical University (Nanjing, Jiangsu, PR China), and it was performed in compliance with the Declaration of Helsinki Principles. Written informed consent was obtained for all patient samples.

Cell Lines

Three human GC cell lines (BGC-823, SGC-7901, and MGC803) and a normal gastric epithelium cell line (GES-1) were purchased from the

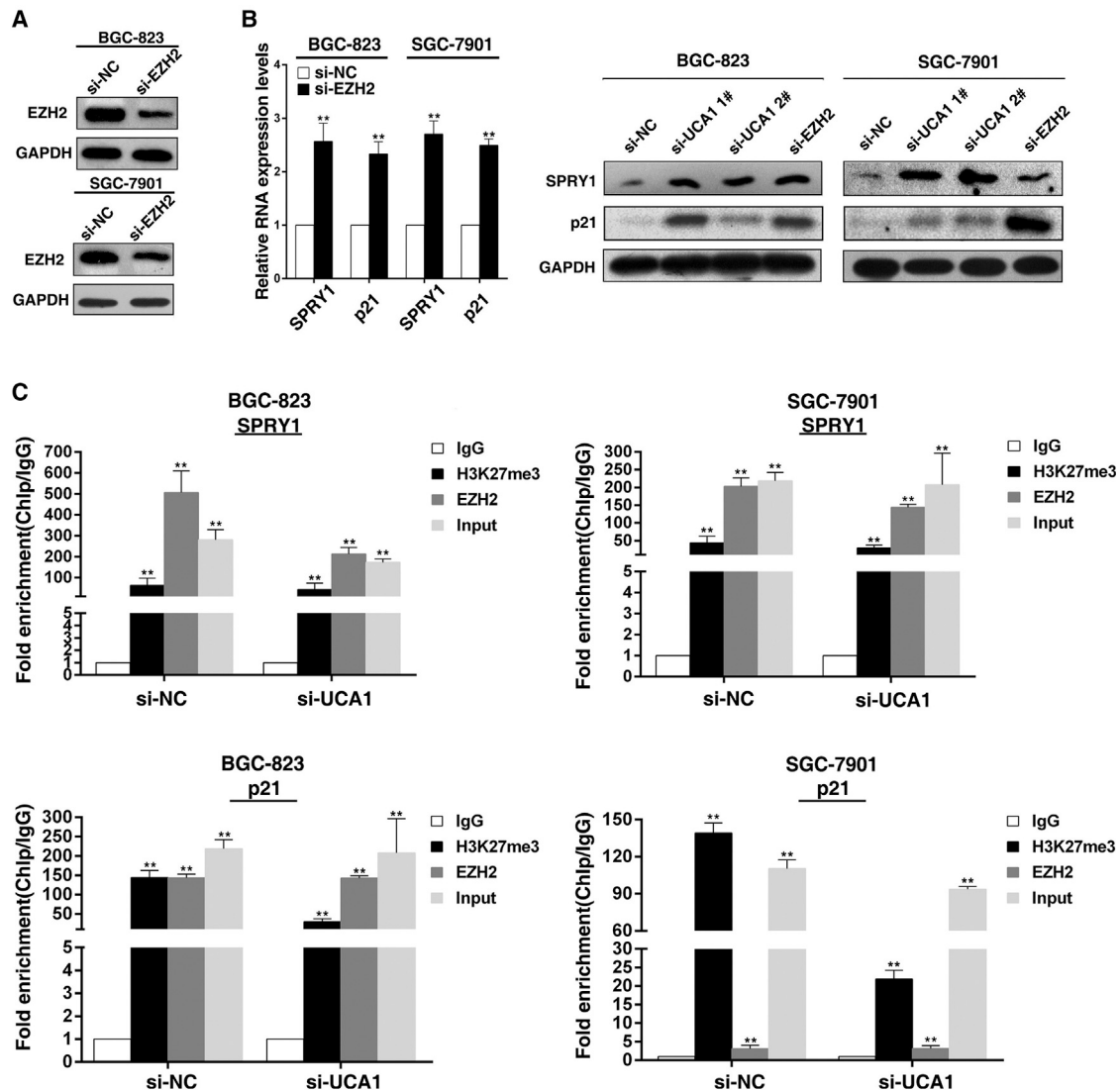


Figure 8. UCA1 Silences the Transcription of p21 and SPRY1 through Binding to EZH2

(A) Relative protein expression levels of EZH2 in BGC-823 and SGC-7901 cells transfected with si-NC or si-EZH2. (B) Relative mRNA levels of p21 and SPRY1 in BGC-823 and SGC-7901 cells transfected with si-NC or si-UCA1. Western blot assays detected the expression of p21 and SPRY1 after knock down of UCA1/EZH2 in BGC-823 and SGC-7901 cells. (C) ChIP-qPCR of EZH2 discern and H3K27me3 binding in the p21 and SPRY1 promoter in two gastric cancer cell lines. * $p < 0.05$, ** $p < 0.01$.

Institute of Biochemistry and Cell Biology of the Chinese Academy of Sciences (Shanghai, China). BGC-823 and MGC803 cells were cultured in RPMI 1640; SGC-7901 cells were cultured in DMEM (Gibco-BRL), supplemented with 10% fetal bovine serum (FBS), 100 U/mL penicillin, and 100 mg/mL streptomycin (Invitrogen, Carlsbad, CA, USA) at 37°C and 5% CO₂.

RNA Extraction and qPCR Assays

Total RNA was isolated with Trizol reagent (Invitrogen) according to the manufacturer's instructions. Total RNA (1 μg) was reverse transcribed in a final volume of 20 μL under standard conditions for the PrimeScript RT reagent Kit (TaKaRa, Dalian, China). SYBR Premix

Ex Taq (TaKaRa, Dalian, China) was used to determine UCA1 and targets' expression levels, following the manufacturer's instructions. Results were normalized to the expression of glyceraldehyde-3-phosphate dehydrogenase (GAPDH). The specific primers are shown in Table S3.

Cell Transfection

GC cells were transfected with siRNAs and plasmid vectors using Lipofectamine 2000 (Invitrogen, USA), in accordance with the manufacturer's protocol. Three individual UCA1 siRNAs and scrambled negative control siRNA (si-NC) were purchased from Invitrogen. The nucleotide sequences of siRNAs for UCA1 and EZH2 are listed

in [Table S3](#). At 48 h post-transfection, cells were harvested for qRT-PCR or western blot analysis.

Cell Proliferation Analysis

Cell viability was tested with an MTT kit (Sigma) according to the manufacturer's instructions. For the colony formation assay, a certain number of transfected cells were placed in each well of 6-well plates and maintained in proper media containing 10% FBS for 2 weeks, during which the medium was replaced every 4 days. Colonies were then fixed with methanol and stained with 0.1% crystal violet (Sigma) in PBS for 15 min. Colony formation was determined by counting the number of stained colonies. For the EdU incorporation assay, cells were cultured in 24-well plates; 10 μ M EdU was added to each well, and cells were cultured for an additional 2 h. Then the cells were fixed with 4% formaldehyde for 30 min. After washing, EdU could be detected with a Click-iTR EdU Kit for 30 min, and the cells were stained with DAPI for 10 min and visualized using a fluorescent microscope (Olympus, Tokyo, Japan). The EdU incorporation rate was expressed as the ratio of EdU-positive cells to total DAPI-positive cells (blue cells), which were counted using Image-Pro Plus (IPP) 6.0 software (Media Cybernetics, Bethesda, MD, USA).

Flow Cytometry Analysis

Transfected cells were harvested after 48-h transfection. Then the double staining with fluorescein isothiocyanate (FITC)-Annexin V and propidium iodide was done by the FITC Annexin V Apoptosis Detection Kit (BD Biosciences), according to the manufacturer's recommendations. The cells were analyzed with a flow cytometer (FACScan; BD Biosciences) equipped with Cell Quest software (BD Biosciences). Cells were discriminated into viable cells, dead cells, early apoptotic cells, and apoptotic cells, and then the relative ratio of early apoptotic cells was compared with control transfection from each experiment. Cells for cell cycle analysis were stained with propidium iodide by the CycleTEST PLUS DNA Reagent Kit (BD Biosciences), following the protocol, and analyzed by FACScan. The percentages of cells in G0–G1, S, and G2–M phases were counted and compared.

Cell Migration and Invasion Assays

For cell migration and invasion assays, 24-well transwell chambers with 8- μ m pore size polycarbonate membrane were used (Corning, Corning, NY, USA). Cells were seeded on the top side of the membrane pre-coated with Matrigel (Becton Dickinson, Franklin Lakes, NJ, USA) (without Matrigel for cell migration assay). After incubation for 24 h, cells inside the upper chamber were removed with cotton swabs, while cells on the lower membrane surface were fixed and then stained with 0.5% crystal violet solution. Five random fields were counted in each well.

In Vivo Assay

Athymic male mice were purchased from the Animal Center of the Chinese Academy of Science (Shanghai, China) and maintained in laminar flow cabinets under specific pathogen-free conditions. For cell proliferation assay *in vivo*, BGC-823 cells were stably transfected

with small hairpin RNA (shRNA) and empty vector and harvested from cell culture plates; then cells were xenografted into BALB/c male nude mice. The tumor volumes and weights were measured every 2 days in mice; the tumor volumes were measured as length \times width² \times 0.5. At 16 days after injection, the mice were killed, and tumor weights were measured and used for further analysis. SGC-7901 cells were stably transfected with shRNA and empty vector and harvested from cell culture plates, washed with PBS, and re-suspended at 2×10^7 cells/mL. Suspended cells (0.1 mL) were injected into the tail veins of three mice, which were sacrificed 7 weeks after injection. The lungs were removed and photographed, and visible tumors on the lung surface were counted. This study was carried out in strict accordance with the Guide for the Care and Use of Laboratory Animals of the NIH. Our protocol was approved by the Committee on the Ethics of Animal Experiments of Nanjing Medical University.

RNA-Seq Bioinformatic Analysis

The mRNA sequencing (mRNA-seq) experiments were performed by Novusbio (Shanghai, China). The mRNA-seq library was prepared for sequencing using standard Illumina protocols. Briefly, total RNAs from scrambled or si-UCA1-transfected BGC-823 cells were isolated using TRIzol reagent (Invitrogen). To remove any contaminating genomic DNA, the total RNA was treated with RNase-free DNase I (New England Biolabs, MA, USA). mRNA extraction was performed using Dynabeadsoligo(dT) (Invitrogen Dynal). Superscript II reverse transcriptase (Invitrogen) and random hexamer primers were used to synthesize double-stranded complementary DNAs. To create the mRNA-seq library, the cDNAs were then fragmented by nebulization and the standard Illumina protocol followed. For the data analysis, basecalls were performed using CASAVA. Reads were aligned to the genome using the split read aligner TopHat (version [v.]2.0.7) and Bowtie2, using default parameters. HTSeq was used for estimating abundances.

Subcellular Fractionation Location

The separation of nuclear and cytosolic fractions was performed using the PARIS Kit (Life Technologies, Carlsbad, CA, USA), according to the manufacturer's instructions.

RNA Immunoprecipitation Assays

RIP experiments were performed using a Magna RIP RNA-Binding Protein Immunoprecipitation Kit (Millipore, USA), according to the manufacturer's instructions. Antibody for RIP assays of EZH2 and SUZ12 were from Abcam.

Chromatin Immunoprecipitation Assays

ChIP assays were performed using EZ-CHIP KIT according to the manufacturer's instructions (Millipore, USA). EZH2 was obtained from Abcam. H3 trimethyl Lys 27 antibody, Histone H3, and Acetyl-Histone H3 Lys27 were from Millipore. The ChIP primer sequences are listed in [Table S2](#). Quantification of immunoprecipitated DNA was performed using qPCR. ChIP data were calculated as a percentage relative to the input DNA by the following equation: $2^{[\text{Input Ct} - \text{Target Ct}]} \times 100$ (%).

Western Blot Assay and Antibodies

Cell protein lysates were separated by 10% SDS-PAGE, transferred to 0.22- μ m NC membranes (Sigma), and incubated with specific antibodies. Autoradiograms were quantified by densitometry (Quantity One software; Bio-Rad). GAPDH antibody was used as a control. Anti-EZH2, Anti-P21, and Anti-SPRY1 were from Abcam (Hong Kong, China).

Statistical Analysis

All statistical analyses were performed using SPSS 20.0 software (IBM, SPSS, USA). The significance of differences between groups was estimated by Student's t test, χ^2 test, or Wilcoxon test, as appropriate. OS rates were calculated by the Kaplan-Meier method with the log-rank test applied for comparison. Survival data were evaluated using univariate and multivariate Cox proportional hazards model. Variables with a value of $p < 0.05$ in univariate analysis were used in subsequent multivariate analysis on the basis of Cox regression analyses. Two-sided p values were calculated, and a probability level of 0.05 was chosen for statistical significance.

SUPPLEMENTAL INFORMATION

Supplemental Information can be found online at <https://doi.org/10.1016/j.omtn.2019.09.024>.

AUTHOR CONTRIBUTIONS

Conception and Design, D.M., E.Z., Q.G., and D.Y.; Development of the Methodology, X.H.; Acquisition of Data, X.H., J.W., and L.H.; Writing the Manuscript, X.H.; Administrative, Technical, and Material Support, J.C. and X.L. All authors read and approved the final manuscript.

CONFLICTS OF INTEREST

The authors declare no competing interests.

ACKNOWLEDGMENTS

This work was supported by grants from the National Natural Science Foundation of China (grants 81702266, 81502071, 81401873, and 81772479). This work was also supported by the China Postdoctoral Science Foundation (2017M610339 and 2017M611913), Jiangsu Planned Projects for Postdoctoral Research Funds (1701041A), and Youth Medical Talent Project in Science and Education, Jiangsu Province, China (QNRC2016057 and QNRC2016380). This work was also supported by Provincial Key Projects (201810312017Z). This work was also supported by Science and Technology Project of xuzhou Medical University (2018KJ23).

REFERENCES

- Siegel, R.L., Miller, K.D., and Jemal, A. (2017). Cancer Statistics, 2017. *CA Cancer J. Clin.* 67, 7–30.
- Soerjomataram, I., Lortet-Tieulent, J., Parkin, D.M., Ferlay, J., Mathers, C., Forman, D., and Bray, F. (2012). Global burden of cancer in 2008: a systematic analysis of disability-adjusted life-years in 12 world regions. *Lancet* 380, 1840–1850.
- Milne, A.N., Carneiro, F., O'Morain, C., and Offerhaus, G.J. (2009). Nature meets nurture: molecular genetics of gastric cancer. *Hum. Genet.* 126, 615–628.
- Li, D., Liu, X., Zhou, J., Hu, J., Zhang, D., Liu, J., Qiao, Y., and Zhan, Q. (2017). Long noncoding RNA HULC modulates the phosphorylation of YB-1 through serving as a scaffold of extracellular signal-regulated kinase and YB-1 to enhance hepatocarcinogenesis. *Hepatology* 65, 1612–1627.
- Chen, Z.Z., Huang, L., Wu, Y.H., Zhai, W.J., Zhu, P.P., and Gao, Y.F. (2016). LncSox4 promotes the self-renewal of liver tumour-initiating cells through Stat3-mediated Sox4 expression. *Nat. Commun.* 7, 12598.
- Mattick, J.S., and Rinn, J.L. (2015). Discovery and annotation of long noncoding RNAs. *Nat. Struct. Mol. Biol.* 22, 5–7.
- Ørom, U.A., and Shiekhattar, R. (2013). Long noncoding RNAs usher in a new era in the biology of enhancers. *Cell* 154, 1190–1193.
- G Hendrickson, D., Kelley, D.R., Tenen, D., Bernstein, B., and Rinn, J.L. (2016). Widespread RNA binding by chromatin-associated proteins. *Genome Biol.* 17, 28.
- Marchese, F.P., Raimondi, I., and Huarte, M. (2017). The multidimensional mechanisms of long noncoding RNA function. *Genome Biol.* 18, 206.
- Marques Howarth, M., Simpson, D., Ngok, S.P., Nieves, B., Chen, R., Siprashvili, Z., Vaka, D., Breese, M.R., Crompton, B.D., Alexe, G., et al. (2014). Long noncoding RNA EWSAT1-mediated gene repression facilitates Ewing sarcoma oncogenesis. *J. Clin. Invest.* 124, 5275–5290.
- Yang, Y., Chen, L., Gu, J., Zhang, H., Yuan, J., Lian, Q., Lv, G., Wang, S., Wu, Y., Yang, Y.T., et al. (2017). Recurrently deregulated lncRNAs in hepatocellular carcinoma. *Nat. Commun.* 8, 14421.
- Rigoutsos, I., Lee, S.K., Nam, S.Y., Anfossi, S., Pasculli, B., Pichler, M., Jing, Y., Rodriguez-Aguayo, C., Telonis, A.G., Rossi, S., et al. (2017). N-BLR, a primate-specific non-coding transcript leads to colorectal cancer invasion and migration. *Genome Biol.* 18, 98.
- Xu, M.D., Wang, Y., Weng, W., Wei, P., Qi, P., Zhang, Q., Tan, C., Ni, S.J., Dong, L., Yang, Y., et al. (2017). A Positive Feedback Loop of lncRNA-PVT1 and FOXM1 Facilitates Gastric Cancer Growth and Invasion. *Clin. Cancer Res.* 23, 2071–2080.
- Zhang, E.B., Kong, R., Yin, D.D., You, L.H., Sun, M., Han, L., Xu, T.P., Xia, R., Yang, J.S., De, W., and Chen, Jf. (2014). Long noncoding RNA ANRIL indicates a poor prognosis of gastric cancer and promotes tumor growth by epigenetically silencing of miR-99a/miR-449a. *Oncotarget* 5, 2276–2292.
- Wang, X.S., Zhang, Z., Wang, H.C., Cai, J.L., Xu, Q.W., Li, M.Q., Chen, Y.C., Qian, X.P., Lu, T.J., Yu, L.Z., et al. (2006). Rapid identification of UCA1 as a very sensitive and specific unique marker for human bladder carcinoma. *Clin. Cancer Res.* 12, 4851–4858.
- Nie, W., Ge, H.J., Yang, X.Q., Sun, X., Huang, H., Tao, X., Chen, W.S., and Li, B. (2016). LncRNA-UCA1 exerts oncogenic functions in non-small cell lung cancer by targeting miR-193a-3p. *Cancer Lett.* 371, 99–106.
- Hu, J.J., Song, W., Zhang, S.D., Shen, X.H., Qiu, X.M., Wu, H.Z., Gong, P.H., Lu, S., Zhao, Z.J., He, M.L., and Fan, H. (2016). Hbx-upregulated lncRNA UCA1 promotes cell growth and tumorigenesis by recruiting EZH2 and repressing p27Kip1/CDK2 signaling. *Sci. Rep.* 6, 23521.
- Bian, Z., Jin, L., Zhang, J., Yin, Y., Quan, C., Hu, Y., Feng, Y., Liu, H., Fei, B., Mao, Y., et al. (2016). LncRNA-UCA1 enhances cell proliferation and 5-fluorouracil resistance in colorectal cancer by inhibiting miR-204-5p. *Sci. Rep.* 6, 23892.
- Qian, Y., Liu, D., Cao, S., Tao, Y., Wei, D., Li, W., Li, G., Pan, X., and Lei, D. (2017). Upregulation of the long noncoding RNA UCA1 affects the proliferation, invasion, and survival of hypopharyngeal carcinoma. *Mol. Cancer* 16, 68.
- Wang, Z.Q., Cai, Q., Hu, L., He, C.Y., Li, J.F., Quan, Z.W., Liu, B.Y., Li, C., and Zhu, Z.G. (2017). Long noncoding RNA UCA1 induced by SP1 promotes cell proliferation via recruiting EZH2 and activating AKT pathway in gastric cancer. *Cell Death Dis.* 8, e2839.
- Zhao, H., Zhang, K., Wang, T., Cui, J., Xi, H., Wang, Y., Song, Y., Zhao, X., Wei, B., and Chen, L. (2018). Long non-coding RNA AFAP1-antisense RNA 1 promotes the proliferation, migration and invasion of gastric cancer cells and is associated with poor patient survival. *Oncol. Lett.* 15, 8620–8626.
- Xu, T.P., Wang, W.Y., Ma, P., Shuai, Y., Zhao, K., Wang, Y.F., Li, W., Xia, R., Chen, W.M., Zhang, E.B., and Shu, Y.Q. (2018). Upregulation of the long noncoding RNA FOXD2-AS1 promotes carcinogenesis by epigenetically silencing EphB3 through EZH2 and LSD1, and predicts poor prognosis in gastric cancer. *Oncogene* 37, 5020–5036.

23. Li, J., Han, L., Roebuck, P., Diao, L., Liu, L., Yuan, Y., Weinstein, J.N., and Liang, H. (2015). TANRIC: An Interactive Open Platform to Explore the Function of lncRNAs in Cancer. *Cancer Res.* 75, 3728–3737.
24. Daa, T., Kashima, K., Kondo, Y., Yada, N., Suzuki, M., and Yokoyama, S. (2008). Aberrant methylation in promoter regions of cyclin-dependent kinase inhibitor genes in adenoid cystic carcinoma of the salivary gland. *APMIS* 116, 21–26.
25. Zhang, Q., Wei, T., Shim, K., Wright, K., Xu, K., Palka-Hamblin, H.L., Jurkevich, A., and Khare, S. (2016). Atypical role of sprouty in colorectal cancer: sprouty repression inhibits epithelial-mesenchymal transition. *Oncogene* 35, 3151–3162.
26. Marchese, F.P., and Huarte, M. (2014). Long non-coding RNAs and chromatin modifiers: their place in the epigenetic code. *Epigenetics* 9, 21–26.
27. Kotake, Y., Nakagawa, T., Kitagawa, K., Suzuki, S., Liu, N., Kitagawa, M., and Xiong, Y. (2011). Long non-coding RNA ANRIL is required for the PRC2 recruitment to and silencing of p15(INK4B) tumor suppressor gene. *Oncogene* 30, 1956–1962.
28. Zhang, E.B., Yin, D.D., Sun, M., Kong, R., Liu, X.H., You, L.H., Han, L., Xia, R., Wang, K.M., Yang, J.S., et al. (2014). P53-regulated long non-coding RNA TUG1 affects cell proliferation in human non-small cell lung cancer, partly through epigenetically regulating HOXB7 expression. *Cell Death Dis.* 5, e1243.
29. Cao, R., Wang, L., Wang, H., Xia, L., Erdjument-Bromage, H., Tempst, P., Jones, R.S., and Zhang, Y. (2002). Role of histone H3 lysine 27 methylation in Polycomb-group silencing. *Science* 298, 1039–1043.
30. Khalil, A.M., Guttman, M., Huarte, M., Garber, M., Raj, A., Rivea Morales, D., Thomas, K., Presser, A., Bernstein, B.E., van Oudenaarden, A., et al. (2009). Many human large intergenic noncoding RNAs associate with chromatin-modifying complexes and affect gene expression. *Proc. Natl. Acad. Sci. USA* 106, 11667–11672.
31. Margueron, R., and Reinberg, D. (2011). The Polycomb complex PRC2 and its mark in life. *Nature* 469, 343–349.
32. Yin, Y., Yan, P., Lu, J., Song, G., Zhu, Y., Li, Z., Zhao, Y., Shen, B., Huang, X., Zhu, H., et al. (2015). Opposing Roles for the lncRNA Haunt and Its Genomic Locus in Regulating HOXA Gene Activation during Embryonic Stem Cell Differentiation. *Cell Stem Cell* 16, 504–516.
33. Spurlock, C.F., 3rd, Tossberg, J.T., Guo, Y., Collier, S.P., Crooke, P.S., 3rd, and Aune, T.M. (2015). Expression and functions of long noncoding RNAs during human T helper cell differentiation. *Nat. Commun.* 6, 6932.
34. Zhang, E., Han, L., Yin, D., He, X., Hong, L., Si, X., Qiu, M., Xu, T., De, W., Xu, L., et al. (2017). H3K27 acetylation activated-long non-coding RNA CCAT1 affects cell proliferation and migration by regulating SPRY4 and HOXB13 expression in esophageal squamous cell carcinoma. *Nucleic Acids Res.* 45, 3086–3101.
35. Lu, X., Huang, C., He, X., Liu, X., Ji, J., Zhang, E., Wang, W., and Guo, R. (2017). A Novel Long Non-Coding RNA, SOX21-AS1, Indicates a Poor Prognosis and Promotes Lung Adenocarcinoma Proliferation. *Cell. Physiol. Biochem.* 42, 1857–1869.
36. Liu, X.H., Sun, M., Nie, F.Q., Ge, Y.B., Zhang, E.B., Yin, D.D., Kong, R., Xia, R., Lu, K.H., Li, J.H., et al. (2014). Lnc RNA HOTAIR functions as a competing endogenous RNA to regulate HER2 expression by sponging miR-331-3p in gastric cancer. *Mol. Cancer* 13, 92.
37. Zhang, E., He, X., Zhang, C., Su, J., Lu, X., Si, X., Chen, J., Yin, D., Han, L., and De, W. (2018). A novel long noncoding RNA HOXC-AS3 mediates tumorigenesis of gastric cancer by binding to YBX1. *Genome Biol.* 19, 154.
38. El-Deiry, W.S. (2016). p21(WAF1) Mediates Cell-Cycle Inhibition, Relevant to Cancer Suppression and Therapy. *Cancer Res.* 76, 5189–5191.
39. Gartel, A.L., and Radhakrishnan, S.K. (2005). Lost in transcription: p21 repression, mechanisms, and consequences. *Cancer Res.* 65, 3980–3985.
40. Sherr, C.J., and Roberts, J.M. (1999). CDK inhibitors: positive and negative regulators of G1-phase progression. *Genes Dev.* 13, 1501–1512.
41. Thaler, S., Hähnel, P.S., Schad, A., Dammann, R., and Schuler, M. (2009). RASSF1A mediates p21Cip1/Waf1-dependent cell cycle arrest and senescence through modulation of the Raf-MEK-ERK pathway and inhibition of Akt. *Cancer Res.* 69, 1748–1757.
42. Fan, T., Jiang, S., Chung, N., Alikhan, A., Ni, C., Lee, C.C., and Hornyak, T.J. (2011). EZH2-dependent suppression of a cellular senescence phenotype in melanoma cells by inhibition of p21/CDKN1A expression. *Mol. Cancer Res.* 9, 418–429.
43. Fritzsche, S., Kenzelmann, M., Hoffmann, M.J., Müller, M., Engers, R., Gröne, H.J., and Schulz, W.A. (2006). Concomitant down-regulation of SPRY1 and SPRY2 in prostate carcinoma. *Endocr. Relat. Cancer* 13, 839–849.
44. Lo, T.L., Yusoff, P., Fong, C.W., Guo, K., McCaw, B.J., Phillips, W.A., Yang, H., Wong, E.S., Leong, H.F., Zeng, Q., et al. (2004). The ras/mitogen-activated protein kinase pathway inhibitor and likely tumor suppressor proteins, sprouty 1 and sprouty 2 are deregulated in breast cancer. *Cancer Res.* 64, 6127–6136.
45. Kwabi-Addo, B., Ren, C., and Ittmann, M. (2009). DNA methylation and aberrant expression of Sprouty1 in human prostate cancer. *Epigenetics* 4, 54–61.
46. Kwabi-Addo, B., Wang, J., Erdem, H., Vaid, A., Castro, P., Ayala, G., and Ittmann, M. (2004). The expression of Sprouty1, an inhibitor of fibroblast growth factor signal transduction, is decreased in human prostate cancer. *Cancer Res.* 64, 4728–4735.
47. Masoumi-Moghaddam, S., Amini, A., Ehteda, A., Wei, A.Q., and Morris, D.L. (2014). The expression of the Sprouty 1 protein inversely correlates with growth, proliferation, migration and invasion of ovarian cancer cells. *J. Ovarian Res.* 7, 61.
48. Calvisi, D.F., Ladu, S., Gorden, A., Farina, M., Lee, J.S., Conner, E.A., Schroeder, L., Factor, V.M., and Thorgeirsson, S.S. (2007). Mechanistic and prognostic significance of aberrant methylation in the molecular pathogenesis of human hepatocellular carcinoma. *J. Clin. Invest.* 117, 2713–2722.
49. Viré, E., Brenner, C., Deplus, R., Blanchon, L., Fraga, M., Didelot, C., Morey, L., Van Eynde, A., Bernard, D., Vanderwinden, J.M., et al. (2006). The Polycomb group protein EZH2 directly controls DNA methylation. *Nature* 439, 871–874.
50. Fahrner, J.A., Eguchi, S., Herman, J.G., and Baylin, S.B. (2002). Dependence of histone modifications and gene expression on DNA hypermethylation in cancer. *Cancer Res.* 62, 7213–7218.
51. Molnar, C., Heinen, J.P., Reina, J., Llamazares, S., Palumbo, E., Breschi, A., Gay, M., Villarreal, L., Vilaseca, M., Pollarolo, G., and Gonzalez, C. (2019). The histone code reader PHD finger protein 7 controls sex-linked disparities in gene expression and malignancy in *Drosophila*. *Sci. Adv.* 5, eaaw7965.
52. Hua, J.T., Ahmed, M., Guo, H., Zhang, Y., Chen, S., Soares, F., Lu, J., Zhou, S., Wang, M., Li, H., et al. (2018). Risk SNP-Mediated Promoter-Enhancer Switching Drives Prostate Cancer through lncRNA PCAT19. *Cell* 174, 564–575.e18.